

An Achromatic Optics for the Linac 2 to Booster Transfer Line

K. Hanke

Abstract

This paper is a summary of simulations and experiments carried out in order to understand the optics of the transfer line from the CERN proton linac (Linac 2) to the CERN PS Booster (PSB). As a result of the studies, a cable inversion between two quadrupoles could be identified and the optics of this transfer line is now fully understood. The model of the line has been used to match an achromatic optics, which was successfully put in place in 2005. The new optics has improved significantly the injection efficiency into the PSB and is beneficial for high brilliance LHC type beams.

Geneva, Switzerland

January 10, 2006

1 Introduction

The optics of the transfer line from the CERN proton linac (Linac 2) to the CERN PS Booster (PSB) has been subject to studies during many years. The longitudinal and transverse emittance can be measured in dedicated measurement lines (LBE, LTE, LTL) and be adjusted to the target match. The dispersion is measured by changing the beam momentum and observing the displacement of the beam center as a function of the momentum at all pick-ups along the line. In the past, simulations of the dispersion agreed qualitatively with experiments but had to be scaled with an artificially introduced factor (the momentum variation had to be multiplied by a factor of 2) in order to achieve quantitative agreement [1].

In the years 1999-2000, a renewed effort was made to debug the model used to simulate the optics parameters (Twiss parameters and dispersion) along the line. The model was verified by means of transfer matrix measurements [2]. At the time, good agreement between model and experiment was only found for matrix elements in the vertical plane, while the horizontal values disagreed. It was furthermore tried to measure the dispersion. The measurements of the horizontal dispersion were not conclusive, while the vertical dispersion was confirmed to be zero all along the line.

In 2002, a new attempt was made to fix the remaining uncertainties involved in the simulation of the line. This implied a renewed cross check of the element positions in the input files for the simulation codes versus the survey data, as well as a verification of the quadrupole settings and the conversion factors from gradient to current. Several bugs could be fixed, and a renewed transfer matrix measurement was performed. It was found, that still a systematic scaling factor of 1.22 was needed to achieve good agreement between calculated and measured matrix elements [3]. It could not be confirmed whether this factor was due to a mis-calibration of the dipole deflection angles or due to the pick-up read-out, but the discrepancy was constant for all matrix elements and hence systematic.

Also in 2002, the dispersion measurements were resumed after having re-calibrated the LBS spectrometer line [4] and the debuncher LT.CDB10 [5]. Qualitative agreement of the horizontal dispersion function along the line with the simulation was found for the nominal¹ optics. However, a scaling factor of 1.75 was needed to achieve quantitative agreement [6].

In 2003, an intense effort was undertaken to sort out all problems in understanding the transfer line optics. For the first time, a conclusive dispersion measurement was performed for the nominal optics, in which simulation and experiment were in perfect agreement without introducing any scaling factors. It remained unclear, why the scaling factor observed in previous measurements had disappeared. An achromatic line was matched using MAD [7], but loading the new settings to the quadrupoles resulted in heavy beam loss and the measured dispersion was found in disagreement with the simulations. The reason for this discrepancy between model and experiment in the case of the matched optics was unclear at the time [8].

This paper summarizes the work done in 2004 and 2005, which led to the discovery of a cabling inversion of two quadrupoles in the LT line. Identifying and fixing the cabling error allowed finally to understand the optics of the line and put in place an achromatic optics. After giving a brief introduction into the parameters and problematics of this transfer line, simulations and experimental results are presented which lead to the conclusion that the optics of the line is now fully understood. First operational experience with the new injection line optics is reported.

¹The optics used until 2005 is referred to as the “nominal” optics.

2 The LT-LTB-BI Line

The Linac 2 to Booster transfer line is composed out of three parts. The LT line starts at the exit of the linac and provides the measurement lines LBE for the transverse and LTE for the longitudinal emittance. The beam is directed into these two measurement lines by the bending magnet LT.BHZ10, which is not used during normal operation and hence does not generate dispersion. The beam is then horizontally deflected by the bending magnets LT.BHZ20 and LT.BHZ30, generating horizontal dispersion. The element LT.BHZ30 marks the end of the LT line (Figure 1).

Starting from element LT.BHZ30, the line is called LTB. This part is a straight line. The beam can be deflected towards two measurement lines, LBE for the transverse emittance and LTE for the longitudinal emittance (Figure 2).

The part of the line between the LTB and the PS Booster is called BI. It provides quadrupoles for the final matching of the beam into the PSB.

The beam from Linac 2 is a 50 MeV proton beam (311 MeV/c) with a nominal beam current of about 160-170 mA. Space charge forces are present, which decrease along the line due to debunching.

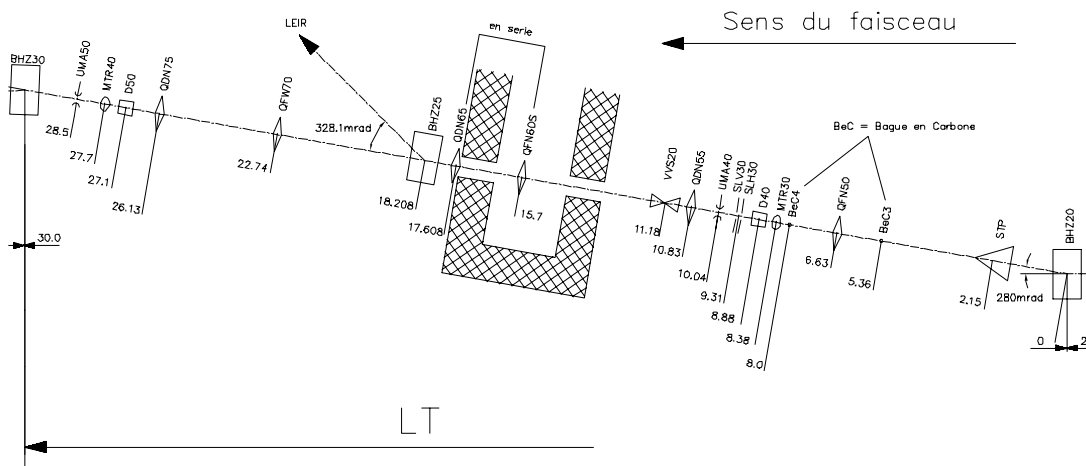
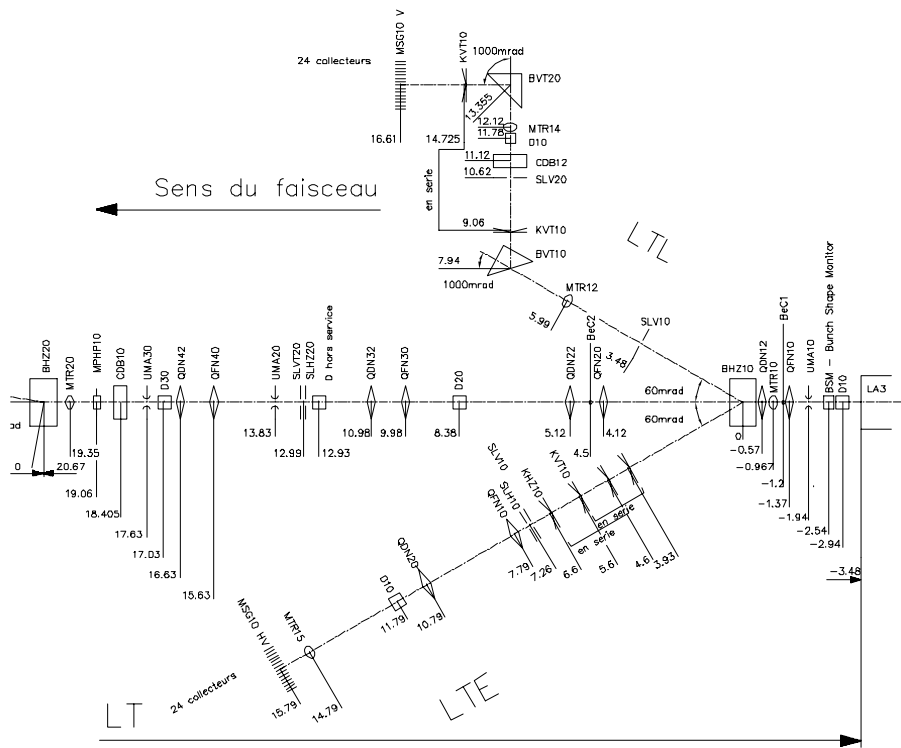


Figure 1: LT line with measurement lines LTE (transverse emittance) and LTL (longitudinal emittance). The beam direction is from right to left and top figure to bottom figure, starting at the exit of tank 3 of Linac 2 (LA3). The beam is horizontally deflected by the bending magnets LT.BHZ20 and LT.BHZ30.

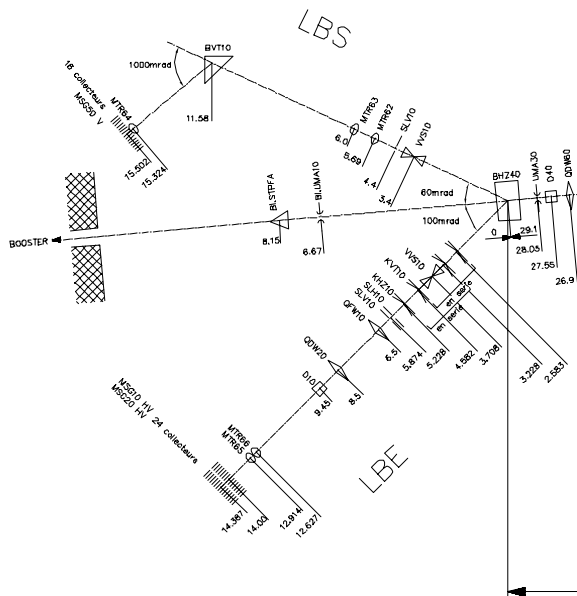
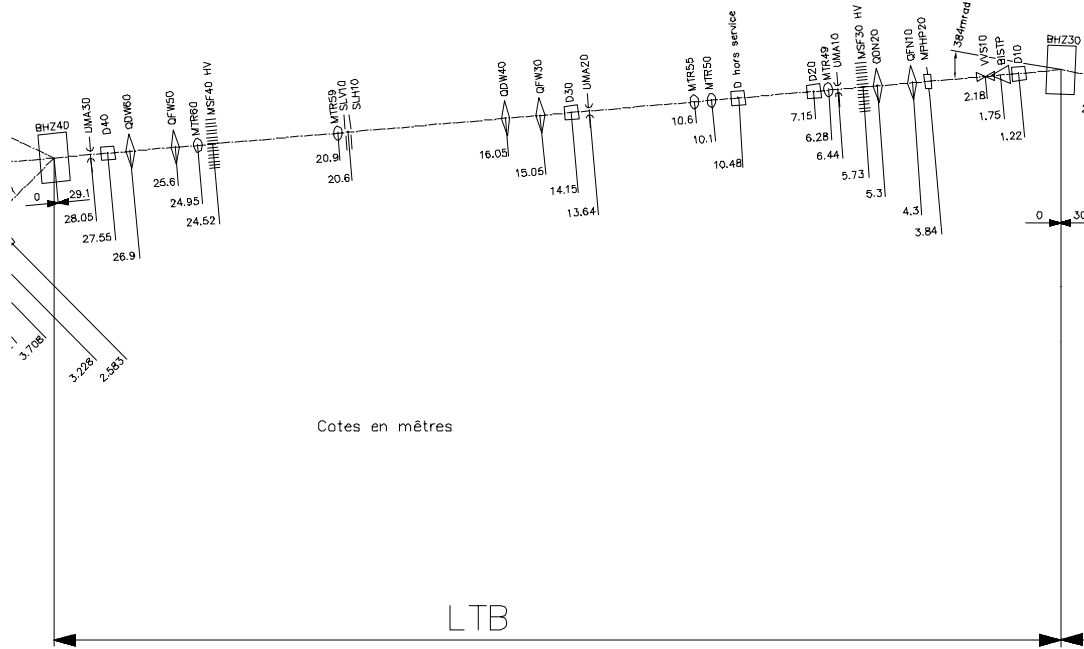


Figure 2: LTB line with measurement lines LBE (transverse emittance) and LBS (beam energy). The beam direction is from right to left and top figure to bottom figure, starting at LT.BHZ30. From the LTB line, the beam goes via the Booster Injection (BI) line into the PS Booster.

3 Dispersion Measurement

The dispersion is measured by changing the beam momentum and observing the corresponding displacement of the beam center at all pick-ups along the line. The beam displacement is recorded for various values of dp/p , averaging over several measurements. The slope of a linear fit is the required dispersion.

The change of beam momentum is accomplished by changing the phase of debuncher LT.CDB10. In order to exclude all uncertainties, first the debuncher LT.CDB10 was re-calibrated in order to determine the momentum change as a function of phase. During this calibration measurement, the beam energy is determined using the LBS spectrometer line, which in turn had been calibrated beforehand [4]. The results of the debuncher calibration are given in Table 1. The various values for the debuncher phase are applied, and the position at the pick-ups along the line read out by an automatic measurement program. The dispersion is obtained off-line using a fitting routine.

LT.CDB10 phase [deg]	dp [keV]	$dp/p (\times 10^{-4})$
285.6	191.7163	6.1645
291.2	122.8243	3.9493
296.8	59.1610	1.9023
302.4*	0.0	0.0
308	-36.9900	-1.1894
313.6	-54.2168	-1.7433
319.2	-76.0086	-2.4440

* reference phase

Table 1: Calibration of debuncher LT.CDB10. The nominal setting is at 302.4 deg, for which dp and dp/p are zero.

4 Simulation of the Line

As will be shown in Section 5, *Space Charge Studies*, the measured dispersion is a space charge independent quantity. In order to simulate the dispersion, two independent codes have been used: MAD [7] and TRACE 3-D [9]. The main difference between these codes is that MAD does not include space charge calculation, while TRACE 3-D can include space charge. For the simulation of the dispersion function, either MAD can be used or TRACE 3-D with the beam current set to zero (no space charge forces). For the simulation of the Twiss parameters and beam envelope, space charge forces have to be taken into account. The simulations presented in the following sections have hence been performed using TRACE 3-D, where for the dispersion matching the beam current has been set to zero, and for the Twiss parameter matching the beam current has been set to 170 mA.

Figure 3 shows a TRACE 3-D simulation of the line with nominal settings. Figure 4 shows again, for the sake of clearness, the horizontal dispersion function as calculated with TRACE 3-D for the nominal optics and zero beam current. The simulation is in excellent agreement with the experimental data.

If the beam current is set to zero in TRACE 3-D, there is good agreement between the MAD and TRACE 3-D simulations. Figure 5 shows the horizontal dispersion calculated both with MAD and with TRACE 3-D. Both codes agree with each other and with the experimental data. It can be concluded, that the measured dispersion is a space charge independent quantity, as only the displacement of the beam center and not the beam size is considered. When using TRACE 3-D to calculate the dispersion, the beam current has to be set to zero in order to have no space charge forces. Else, the dispersion calculated by TRACE 3-D is overestimated. However, when calculating Twiss parameters and beam envelope, space charge must be taken into account and the full beam current used in the simulation.

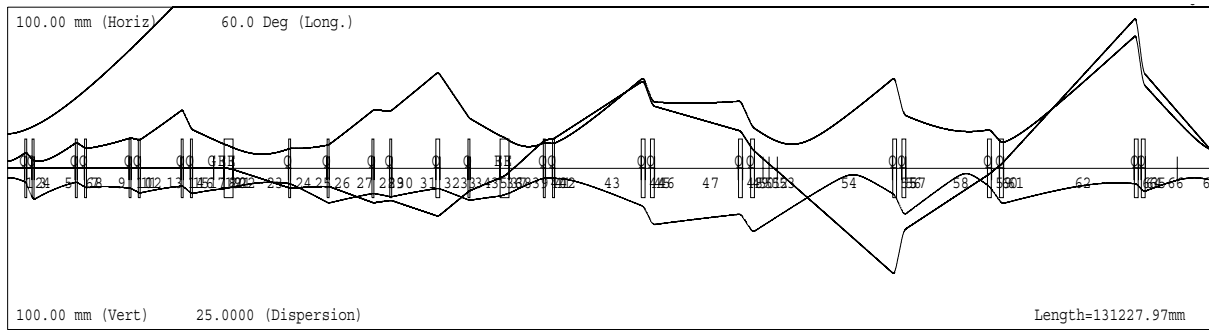


Figure 3: TRACE 3-D simulation of the line with nominal* settings. The upper and lower lines represent the horizontal and vertical envelope (scale 100 mm). The horizontal dispersion starts to develop from the first bending magnet, and arrives at the second bending magnet with $D \approx 0$ but $D' \neq 0$. Consequently, D and D' have non-zero values throughout the rest of the line. The dispersion function is plotted again separately in Fig. 4 for sake of clarity.

* As used until 2005.

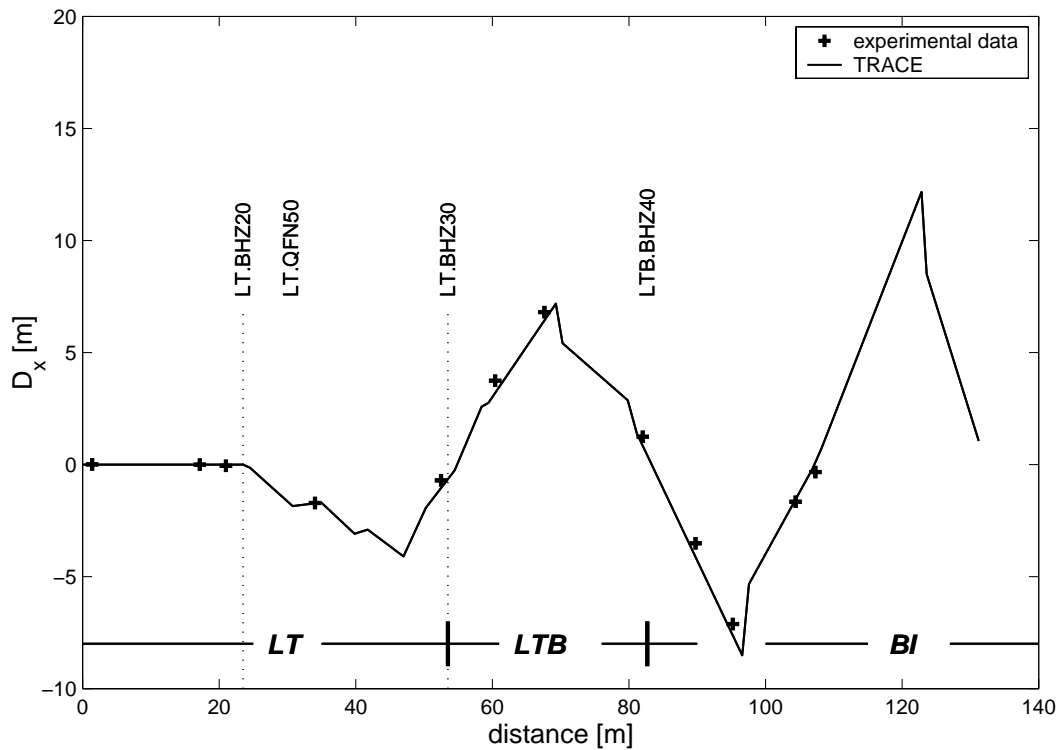


Figure 4: TRACE 3-D simulation of the horizontal dispersion along the line (solid line) and measured dispersion (crosses) for the nominal optics. The beam current in TRACE has been set to zero.

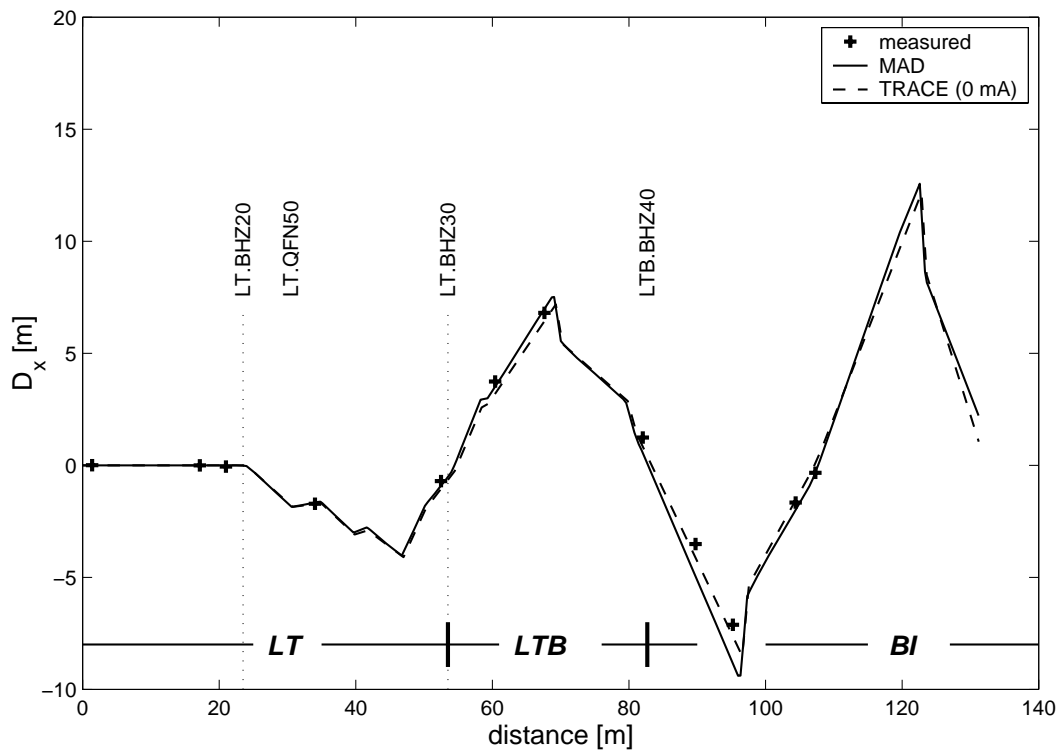


Figure 5: Dispersion along the LT-LTB-BI line calculated with TRACE 3-D (dashed line) and MAD (solid line). Both codes as well as the experimental data are in good agreement.

5 Space Charge Studies

When setting the beam current to 170 mA in TRACE 3-D, the dispersion is overestimated as can be seen in Figure 6. For this case, experimental values and the simulation disagree. Therefore, the beam current has to be set to zero in TRACE 3-D in order to reproduce correctly the measured dispersion.

In order to prove experimentally the independence of the dispersion of space charge, the beam current has been reduced by changing the arc current of the proton source. Table 2 shows the beam current for three different values of the source arc current.

arc current [A]	beam current [mA]
38.45*	170
30	113
20	60

* nominal setting

Table 2: Beam current as function of source arc current as used for space charge studies.

The beam current has been changed according to Table 2 and the dispersion been measured for each setting. Figure 7 shows the measured dispersion for the different beam currents as well as a TRACE 3-D simulation with zero current. All measurements as well as the simulation agree. It has hence experimentally been shown, that the observed quantity is space charge independent.

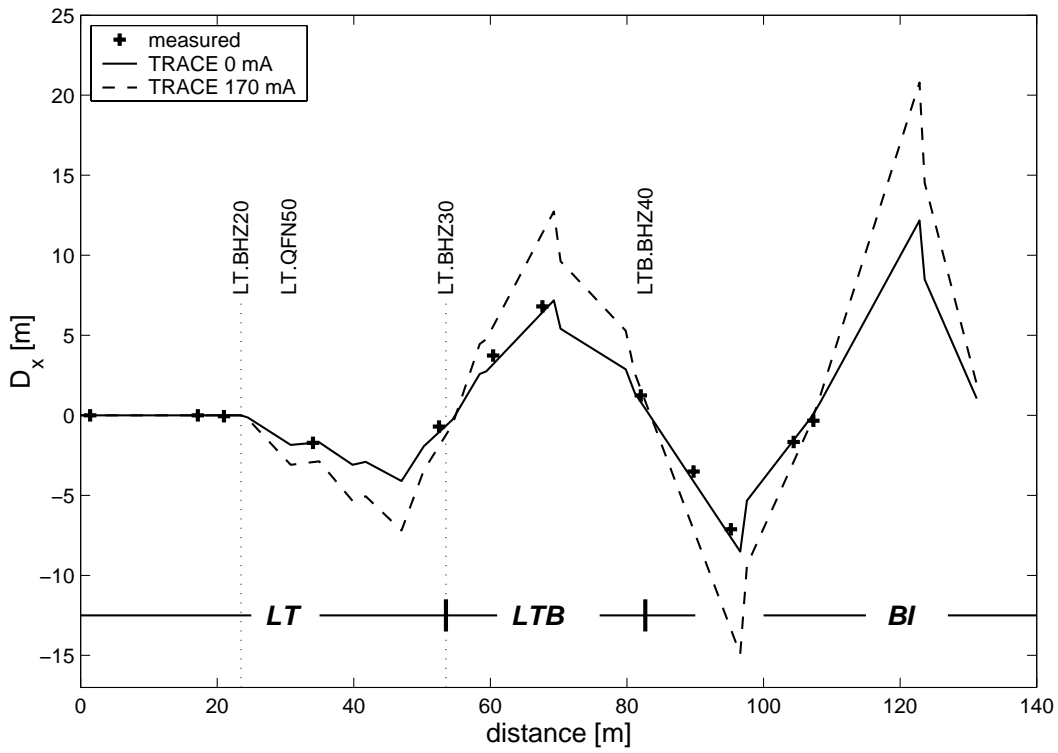


Figure 6: TRACE 3-D simulation of the horizontal dispersion along the LT-LTB-BI line (solid line) and measured dispersion (crosses) for the nominal optics. The beam current in the simulation has been set to 170 mA. The calculated dispersion is overestimated and does not agree with the experimental results.

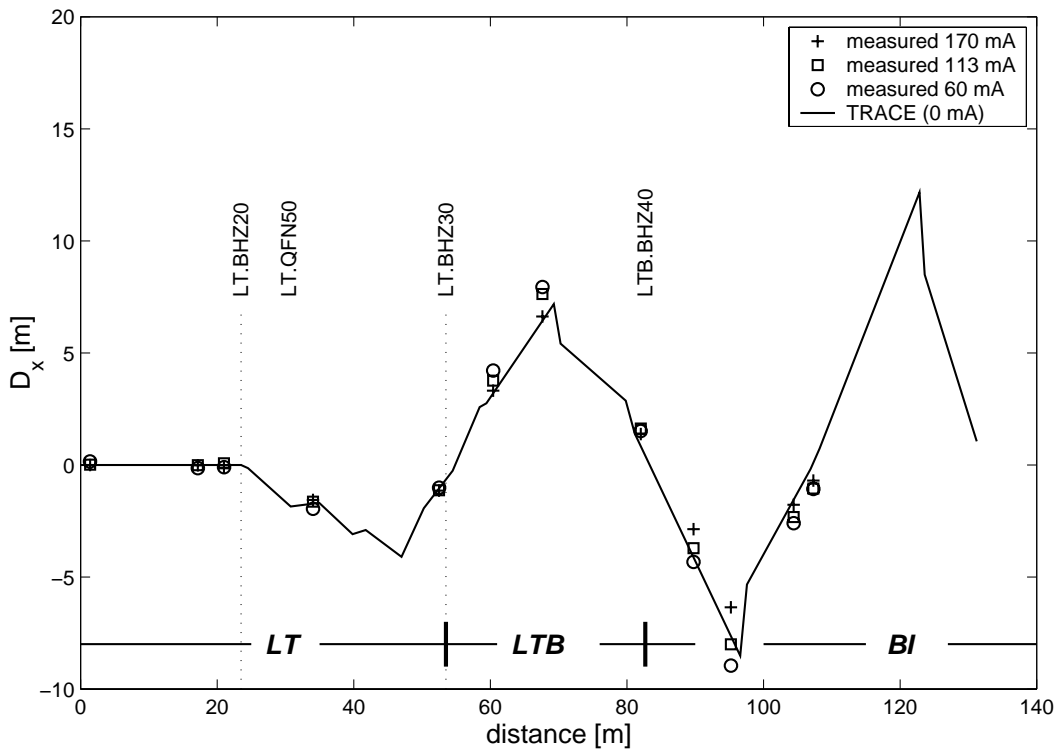


Figure 7: Measured dispersion for three different beam currents and nominal optics. All experimental data agree with a TRACE 3-D simulation, in which the beam current has been set to zero.

6 Matching an Achromatic Optics

The TRACE 3-D model has been used to match both D_x and D'_x to zero at the exit of the second bending (LT.BHZ30). In order to match simultaneously D_x and D'_x , the quadrupoles between the bending magnets LT.BHZ20 and LT.BHZ30 have to be used. Downstream of LT.BHZ30, the dispersion invariant cannot be changed any more and only D_x be traded off against D'_x . If, however, both D_x and D'_x can be nullified (achromatic line), the dispersion function will be zero all along the rest of the line. The quadrupoles downstream of LT.BHZ30 can then be used to re-match the Twiss parameters (the Twiss parameter matching will in general be perturbed when doing the dispersion matching) to their original values at Booster injection.

6.1 Dispersion Matching

Figure 8 shows a TRACE 3-D simulation for an achromatic line. The horizontal dispersion is zero coming from the Linac, and starts to have non-zero values downstream of LT.BHZ20. The first horizontally focusing quadrupole downstream of LT.BHZ20 is used to change the sign of D'_x such that D_x and D'_x arrive at LT.BHZ30 with the correct sign and value such that both are canceled. The dispersion is then close to zero downstream of LT.BHZ30. The envelope and Twiss parameters at Booster injection have been re-matched using quadrupoles downstream of LT.BHZ30. For sake of clearness, Figure 9 shows again the horizontal dispersion along the line for the matched and unmatched case.

While a solution for an achromatic optics existed on paper since a while, loading the calculated settings to the quadrupoles in the line resulted in heavy beam loss and did not have the desired effect on the dispersion. The fact, that the model described well the “nominal” optics, while simulations and experiments disagreed for the matched, achromatic case, was for a long time a mystery. Lengthy investigations were performed, such as measurements with different quadrupole settings, transfer matrix measurements and polarity tests of the quadrupoles. From the various tests, it could be concluded that the problem was localized around LT.QFN50 (the first horizontally focusing quadrupole downstream of LT.BHZ20). This magnet plays a key role in the dispersion matching, as it has to be powered to about twice of its original value in order to flip the sign of D'_x . Having narrowed down the problem to this quadrupole, the hardware was re-checked and a cabling inversion between LT.QFN50 and LT.QDN75 identified. This cabling error had not been noticed for a long time. The magnets had been functioning with their corresponding correct polarities as it had been confirmed before. For the “nominal” optics, their values were reasonably close, which is why simulations and experiments agreed for this optics. However, when powering LT.QFN50 to twice of its original value, the effect on the beam was not at all the desired one. In early 2005, after fixing the cabling inversion, the new optics could for first time be put in place and the dispersion be measured as shown in Fig. 9 [10].

6.2 Twiss Parameter Matching

When matching the D_x and D'_x using quadrupoles between LT.BHZ20 and LT.BHZ30, in general the Twiss parameter matching at Booster injection will be perturbed. The quadrupoles downstream of LT.BHZ30 have hence been used in order to re-match the Twiss parameters to the target match. The target match at the injection septum BI.SMH is shown in Table 3. The left part of the table shows the optics parameters of the beam in the PSB at the center of section 1L1. Note, that the vertical β -function has changed in 2004 with the installation of a new PSB working point [11]. Note also, that in the vertical plane the parameters of PSB and injection line agree, while in the horizontal plane the incoming beam must have a smaller β than the one given by the machine lattice to allow for horizontal stacking.

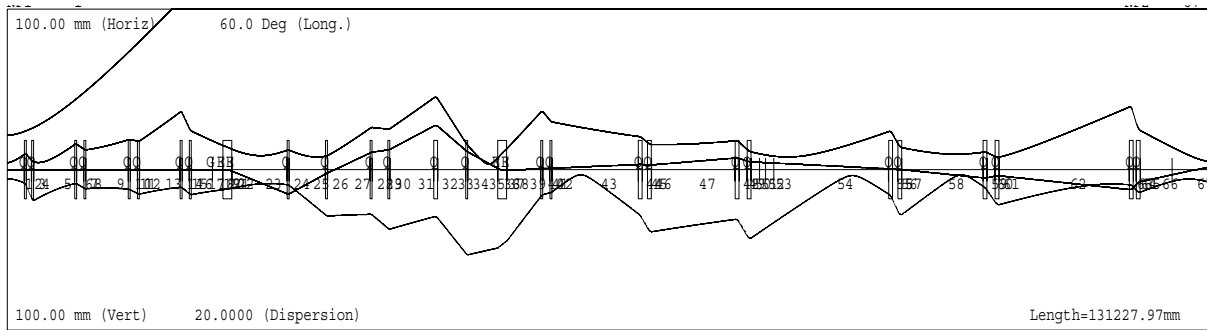


Figure 8: TRACE 3-D simulation of envelope and dispersion along the LT-LTB-BI line for the matched, achromatic optics. While the dispersion is nullified, the beam envelope is well confined.

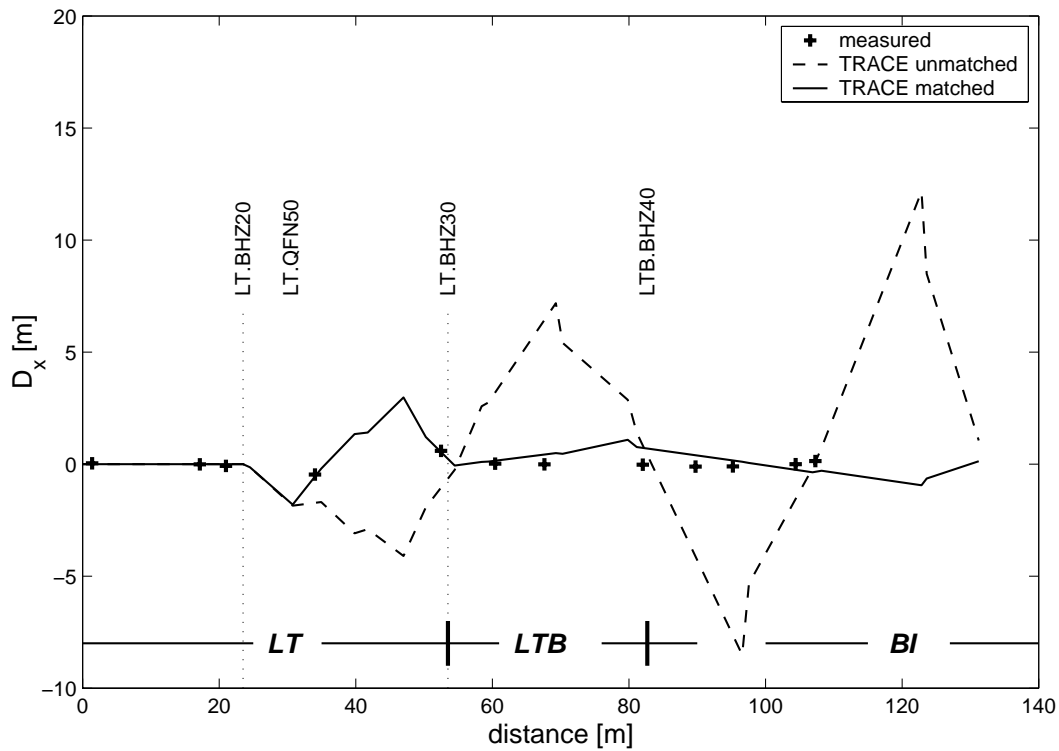


Figure 9: Horizontal dispersion calculated with TRACE 3-D along the line for achromatic optics (solid line) and operational optics (dashed line). For the matched optics, the dispersion changes sign between the two bending magnets and arrives at the second bend such that both D and D' are canceled.

	PSB Ring		Injected Beam	
	horizontal	vertical	horizontal	vertical
α	0.0	0.0	0.0	0.0
β [m]	5.6	4.22*	2.0	4.22
D [m]	1.42	0.0	1.42	0.0
D'	0.0	0.0	0.0	0.0

* New PSB working point $Q_h = 4.17/Q_v = 4.23$ as from 2004. Old value with $Q_h = 4.17/Q_v = 5.23$ was 2.78 m.

Table 3: Target match at injection into the PS Booster.

7 Operational Performance

7.1 Injected Intensity

The new, achromatic optics has significantly increased the injection efficiency into the PSB. While in the past, the injection efficiency had peak values of around 55-60% (for an ISOLDE type beam with about 13 turns injected per ring; the injection efficiency depends on the number of turns injected and decreases with less turns injected), values of 75% and more were observed for this type of beam. This can be understood from the multiturn injection process. A small beam (due to zero dispersion) at the location of the injection septum reduces the losses which occur during the injection process itself as well as during the first turns in the machine. Presently, rings 1 and 2 show very good performance while ring 4 is slightly worse and ring 3 shows comparatively bad performance. The fact that the rings perform differently is not related to the new injection line optics but has been observed also with the old optics. The gain in injected intensity does not translate directly in extracted intensity, as there are further limitations in capture and acceleration efficiency. Nevertheless, careful optimization made it possible to accelerate a total intensity of 4×10^{13} with 13 turns injected per ring during the 2005 run.

7.2 Emittance and Brilliance

While high intensity is an issue for certain users, e.g. the ISOLDE and CNGS beams, other beams require moderate intensity but high brilliance. This is in particular the case for LHC type beams. The standard LHC beam delivered from the PSB in the past provided 150×10^{10} particles per bunch with three turns injected per ring. With the new injection line optics, a given intensity can be injected with less turns, as the injection efficiency is higher than before. For example, an intensity of 150×10^{10} particles per bunch can now be injected with 2 - 2.5 turns/ring (depending on the ring). Table 4 shows the number of injected turns necessary to fill the Booster rings with 150, 200 and 250×10^{10} particles. In the same table, the average transverse emittance $((\epsilon_x + \epsilon_y)/2)$ for the four Booster rings and the different intensities considered is shown. It can be seen, that rings 1,2 and 4 are performing well, while there is a problem with ring 3 which requires more turns for a given intensity and shows consequently a larger emittance.

The new optics is hence not only beneficial for high-intensity beams, but also for beams with moderate intensity and high brilliance. Figures 10 and 11 show the normalized rms emittance measured with the SEM grids in the measurement line (ML) for intensities of 150, 200 and 250×10^{10} particles per bunch. Note, that the total emittance after recombination of the four rings is larger than the emittance of the single rings. This figure can be further optimized by improving the steering in the extraction line.

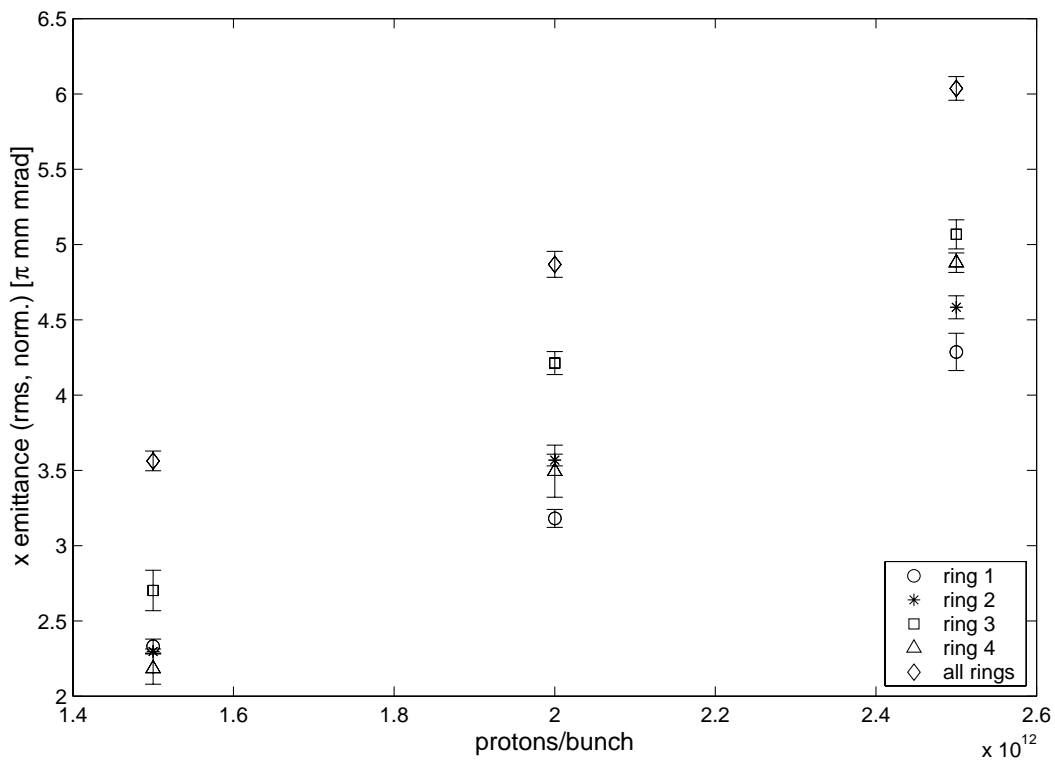


Figure 10: Horizontal emittance (normalized, rms) for all four Booster rings as well as for the total beam composed of the four rings versus intensity per bunch.

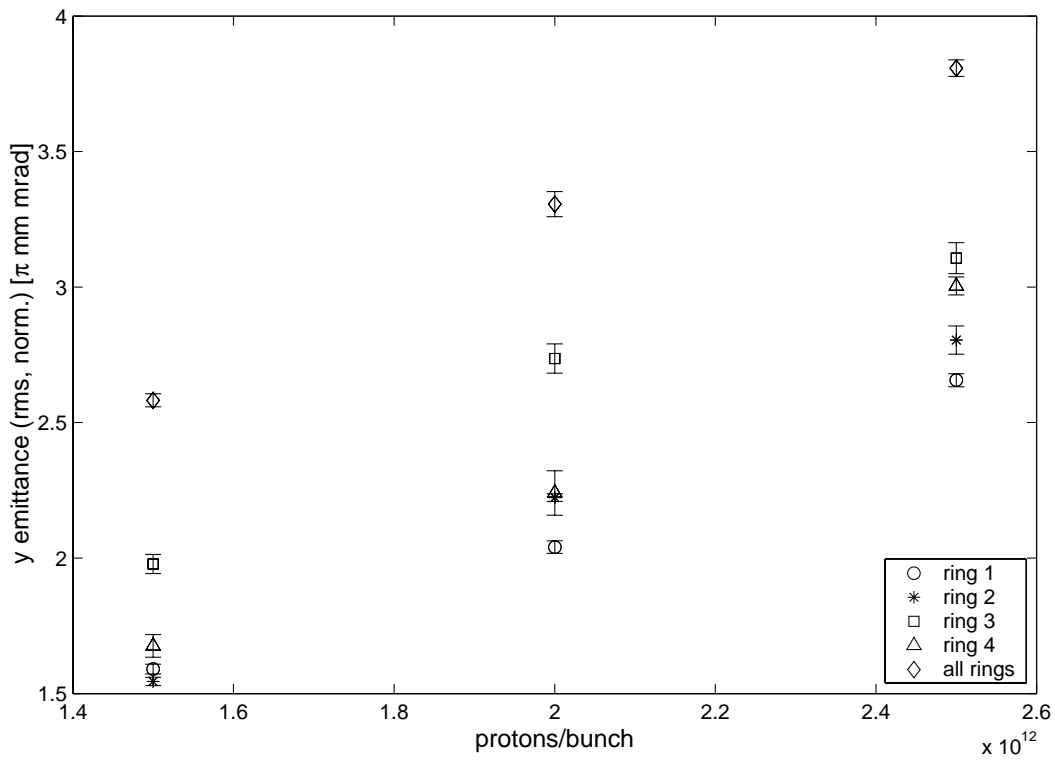


Figure 11: Vertical emittance (normalized, rms) for all four Booster rings as well as for the total beam composed of the four rings versus intensity per bunch.

	150×10^{10} p/bunch		200×10^{10} p/bunch		250×10^{10} p/bunch	
	turns	ε [π mm mrad]	turns	ε [π mm mrad]	turns	ε [π mm mrad]
ring 1	2.2	1.96	2.8	2.61	3.5	3.47
ring 2	2.2	1.92	3.0	2.90	3.5	3.69
ring 3	3.2	2.34	4.0	3.47	5.3	4.09
ring 4	2.3	1.93	3.0	2.87	3.7	3.94

Table 4: Average transverse emittance $(\varepsilon_x + \varepsilon_y)/2$ for the four Booster rings and the different intensities considered.

8 Conclusions

A new, achromatic injection line optics for the CERN PS Booster could successfully be put in place in early 2005, after many years of debugging both simulation codes and transfer line hardware. After a test phase, the optics has been installed for all users and can now be considered operational. As an immediate consequence of the new optics, the injection efficiency into the PSB has increased by about 15-20%. This is not only beneficial high intensity beams for e.g. ISOLDE or CNGS, but also for LHC type beams of high brilliance.

References

- [1] M. Chanel, A. Lombardi, Dispersion Measurements 1996, not published.
- [2] K. Hanke, A. Lombardi, R. Scrivens, *Measurement of the Optics Parameters in the LTB and ITH Lines*, CERN PS-Note-2000-003 PP (2000).
- [3] P. Eliasson, K. Hanke, A. Lombardi, J. Sanchez, R. Scrivens, *Study of the LT-LTB Line via Transfer Matrix Measurements*, CERN PS-Note-2002-107 PP (2002).
- [4] R. Scrivens, Angle and Scan Calibration of the LBS.MSG50 SEM Grid, 2 May 2002, not published.
- [5] R. Scrivens, *Beam Momentum Shift Calibration from the Debuncher (LT.CDB10)*, 16 May 2002, not published.
- [6] P. Eliasson, K. Hanke, R. Scrivens, *Dispersion Measurement of 7 August 2002*, not published.
- [7] MAD Version 8.23/08 Linux.
- [8] K. Hanke, J. Sanchez-Conejo, *Study of the Optics Parameters in the LT-LTB-BI Transfer Line*, CERN AB-Note-2003-092 OP (2003).
- [9] K. R. Crandall, D. P. Rusthoi, *TRACE 3-D Documentation*, LA-UR-97-886 (1997).
- [10] K. Hanke, R. Scrivens, J. Sanchez-Conejo, *Dispersion Matching of a Space-Charge Dominated Beam at Injection into the CERN PS Booster*, conf. proc. PAC2005 and CERN-AB-2005-032 (2005).
- [11] M. Benedikt, A. Blas, C. Carli, M. Chanel, H. Fiebiger, A. Findlay, K. Hanke, J.-L. Sanchez-Alvarez, J. Tan, P. Urschütz, *Study of a New Working Point for the CERN PS Booster*, CERN AB-Note-2004-064 MD (2004).

A Quadrupole Settings

Quadrupole	effective length [m]	current [A] (old optics)	gradient [T/m]	conversion factor
LT.QFN10	0.255	293.00	4.6508	63.00
LT.QDN12	0.255	230.00	3.6508	63.00
LT.QFN20	0.255	130.00	2.0635	63.00
LT.QDN22	0.255	90.00	1.4286	63.00
LT.QFN30	0.255	44.20	0.7016	63.00
LT.QDN32	0.255	73.00	1.1587	63.00
LT.QFN40	0.255	112.50	1.7857	63.00
LT.QDN42	0.255	97.10	1.5413	63.00
LT.QFN50	0.255	45.70	0.7254	63.00
LT.QDN55	0.255	52.40	0.8317	63.00
LT.QFN60	0.255	34.80	0.5524	63.00
LT.QDN65	0.255	34.80	0.5524	63.00
LT.QFW70	0.467	7.50	0.5376	13.89
LT.QDN75	0.255	41.00	0.6508	63.00
LTB.QFN10	0.255	63.00	1.0000	63.00
LTB.QDN20	0.255	32.00	0.5079	63.00
LTB.QFW30	0.461	11.00	0.7885	13.95
LTB.QDW40	0.461	11.00	0.7885	13.95
LTB.QFW50	0.461	10.00	0.7168	13.95
LTB.QDW60	0.461	10.00	0.7168	13.95
BI.QNO10	0.462	16.50	1.1644	14.17
BI.QNO20	0.462	19.20	1.3550	14.17
BI.QNO30	0.462	10.70	0.7551	14.17
BI.QNO40	0.462	14.40	1.0161	14.17
BI1.QNO50	0.466	47.00	1.1700	40.17
BI1.QNO60	0.466	54.00	1.3443	40.17
BI2.QNO50	0.466	48.53	1.2081	40.17
BI2.QNO60	0.466	54.00	1.3443	40.17
BI3.QNO50	0.466	51.50	1.2821	40.17
BI3.QNO60	0.466	56.50	1.4065	40.17
BI4.QNO50	0.466	49.50	1.2323	40.17
BI4.QNO60	0.466	56.50	1.4065	40.17

Table 5: Quadrupole settings for old optics. The lattice is a FODO lattice, where “QF” is a horizontally focusing quadrupole and “QD” a horizontally defocussing quadrupole. The sign in the simulation has to be set accordingly, while it is automatically done in the control system. Note some discrepancies in the notation between the control system and the official names as of 1996.

Quadrupole	effective length [m]	current [A] (new optics)	gradient [T/m]	conversion factor
LT.QFN10	0.255	293.00	4.6508	63.00
LT.DE12	0.255	230.00	3.6508	63.00
LT.QR20	0.255	130.00/125.00*	2.0635	63.00
LT.QDN22	0.255	90.00/85.00*	1.4286	63.00
LT.QFN30	0.255	44.20/47.20*	0.7016	63.00
LT.QDN32	0.255	73.00/57.00*	1.1587	63.00
LT.QFN40	0.255	112.50	1.7857	63.00
LT.QDN42	0.255	97.10	1.5413	63.00
LT.QFN50	0.255	92.97	1.4757	63.00
LT.QDN55	0.255	45.20	0.7174	63.00
LT.QFN60	0.255	45.20	0.7174	63.00
LT.QDN65	0.255	45.20	0.7174	63.00
LT.QFW70	0.467	8.98	0.6462	13.89
LT.QDN75	0.255	41.12	0.6527	63.00
LTB.QFN10	0.255	93.07	1.4773	63.00
LTB.QDN20	0.255	49.57/42.57*	0.7869	63.00
LTB.QFW30	0.461	6.31/7.00*	0.4520	13.95
LTB.QDW40	0.461	9.20/8.90*	0.6592	13.95
LTB.QFW50	0.461	10.29/10.49*	0.7376	13.95
LTB.QDW60	0.461	10.03/11.73*	0.7188	13.95
BI.QNO10	0.462	16.50	1.1644	14.17
BI.QNO20	0.462	19.20	1.3550	14.17
BI.QNO30	0.462	10.70	0.7551	14.17
BI.QNO40	0.462	14.40	1.0161	14.17
BI1.QNO50	0.466	47.00	1.1700	40.17
BI1.QNO60	0.466	54.00	1.3443	40.17
BI2.QNO50	0.466	48.53	1.2081	40.17
BI2.QNO60	0.466	54.00	1.3443	40.17
BI3.QNO50	0.466	51.50	1.2821	40.17
BI3.QNO60	0.466	56.50	1.4065	40.17
BI4.QNO50	0.466	49.50	1.2323	40.17
BI4.QNO60	0.466	56.50	1.4065	40.17

* Some quadrupoles needed manual tuning after putting in place the calculated settings in order to recover full transmission through the line and further optimize the injection efficiency. The values on the left are the calculated settings, the values on the right are the tuned, operational settings. The tuning does not affect the dispersion matching, but acts only on the Twiss parameters whose initial values at the exit of the linac are not perfectly known.

Table 6: Quadrupole settings for new optics. The lattice is a FODO lattice, where “QF” is a horizontally focusing quadrupole and “QD” a horizontally defocussing quadrupole. The sign in the simulation has to be set accordingly, while it is automatically done in the control system. Note some discrepancies in the notation between the control system and the official names as of 1996. Quadrupoles in the BI line were not used for the matching except for some manual fine tuning of the beam at injection into the four rings. These quadrupoles were found to have essentially the same settings as in case of the old optics. Note, that individual rings have slightly different settings for the last two (individual) quadrupoles, i.e. the matching conditions differ slightly from ring to ring.